

## Internal Stress in Nickel Thin Films Affected by Additives in Electrodeposition

M. Saitou

Department of Mechanical Systems Engineering, University of the Ryukyus, 1 Senbaru Nishihara-cho Okinawa, 903-0213, Japan

E-mail: [saitou@tec.u-ryukyu.ac.jp](mailto:saitou@tec.u-ryukyu.ac.jp)

Received: 24 November 2015 / Accepted: 11 December 2015 / Published: 1 January 2016

---

The effect of additives on the internal stress in electrodeposited nickel thin films has been investigated using a bent strip measurement and X-ray diffraction. The additives such as saccharin sodium and p-toluenesulfonamide cause a decrease in the internal stress and a shift from a tensile stress to a compressive stress. The changes in the internal stress are described as a power law deviated from the internal stress in the nickel thin film generated from a solution free of the additive. This indicates that within a framework of the dynamic scaling theory the effect of the additive is equivalent to a quenched noise that disturbs the surface growth by its adsorption on active sites in the nickel thin film. The internal stress is found to be summarized as a unified equation.

---

**Keywords:** internal stress; additive; nickel thin film; dynamic scaling theory; quenched noise; scaling law

### 1. INTRODUCTION

The internal stress in electrodeposited thin films has attracted researchers in science and technology because of the origin of internal stress in films [1] and the film detachment [2] from a substrate. The behavior of internal stress affected by many kinds of parameters in electrodeposition [3] is so complicated that a unified description of the internal stress seems to be impossible. However, the internal stress in nickel thin films electrodeposited using a direct current or alternative pulse current has recently been reported to be written as a unified equation [4]:

$$\sigma \sim \left[ i_f \left( \frac{T_{on}}{T_{on} + T_{off}} \right) \right]^m h^{-n}, \quad (1)$$

where  $i_f$  is the amplitude of current density,  $T_{on}$  and  $T_{off}$  are the current on time and off time,  $m$  is an exponent, and  $n$  is the scaling exponent that characterizes the dynamics of the growth process [5].

For the direct current electrodeposition,  $T_{\text{off}}$  takes a value of zero. Equation (1) indicates that the internal stress involved with phase transition such as the film growth obeys the scaling law as a corollary.

The effect of additives on the internal stress in thin films generated by electrodeposition has been studied for a long time [6-7]. In general, the additive is known to reduce the internal stress [8-11]. However, the internal stress affected by the additive has not been analyzed using the dynamic scaling theory. As shown in Eq. (1), within a framework of the dynamic scaling theory, the internal stress is expected to be described as a unified equation.

A quenched noise [5-6] that does not change with time is derived from inhomogeneity of media in which the surface advances. For example, pores that distributed in a porous media [12], which act as the quenched noise, play a role in the resistance of the moving interface of liquid in the media and cause a pinning-depinning transition. In electrodeposition, an additive that influences the surface roughness of deposits is considered to behave as a quenched noise in the dynamic scaling theory. The additive that usually adsorbs on active sites in the surface randomly distributes and blocks the movement of adatoms such as metal atoms. Hence, the rapid growth at the active site appears to be suppressed by the additive as well as the pore in the porous media.

On the other hand, the quenched noise is found to change the scaling behavior related to surface growth mechanisms. Hence, Eq. (1) may also be modified by the presence of the quenched noise in electrodeposition. Our simple question is what change in the internal stress that obeys the power law occurs when the quenched noise are introduced in film growth.

So as to measure the internal stress in thin films, the bent strip measurement [4] using a curvature deformation of the substrate was applied in comparison with the previous study. The additives used in this study were saccharin sodium and p-toluenesulfonamide known as the levelling additive [9].

In the present study, we demonstrate the effect of the additive on the internal stress in electrodeposited nickel films, and show a unified equation that describes the internal stress.

## 2. EXPERIMENTAL

The experiment was performed in the same way as that in the Reference [4]. The experimental method is called the bent strip measurement. A specimen (Specialty Testing and Development Co. made) consisting of two legs made of beryllium copper alloy was used. Each one side of the two legs was coated with an insulating organic thin film to prevent electrodeposition. The two legs on which nickel was electrodeposited were spread onward or inward corresponding to the tensile or compressive stress in the nickel thin film. The specimen and two poly-crystalline nickel sheets of  $90 \times 60 \times 0.5 \text{ mm}^3$  were prepared for a cathode electrode and anode electrodes.

The cathode and two anode electrodes were put in a bath including ( $\text{gL}^{-1}$ ): nickel sulfamate 600, boric acid 40, saccharin sodium (SS used as an abbreviation in this study) 0,  $18 \times 10^{-3}$ ,  $38 \times 10^{-3}$ ,  $58 \times 10^{-3}$ , and p-toluenesulfonamide (PTSA used as an abbreviation in this study); 0,  $18 \times 10^{-3}$ ,  $38 \times 10^{-3}$ .

The cathode electrode was located in the center of the bath maintained at a temperature of 300 K. The direct current density having a range from 1 to 24 mA cm<sup>-2</sup> were provided with a power supply (Advantest, R6145). After electrodeposition, the specimen on which nickel was electrodeposited was rinsed with distilled water and dried. The changes in the curvature and the weight of the specimen were measured to determine the internal stress.

The nickel thin film on the specimen was investigated to determine a crystallographic plane parallel to the specimen by conventional XRD (Rigaku Ultima) with CuK $\alpha$  radiation using a standard  $\theta$ -2 $\theta$  diffractometer with a monochromator of carbon.

### 3. RESULTS AND DISCUSSION

Statistical surface growth models are generally expressed by Langevin-type equations including the noise [13] that plays an important role in phase transition. When the noise is independent of time and a function of film thickness [14], the noise that usually is a function of time is called a quenched noise has an effect of pinning or depinning a moving interface [15]. In electrodeposition, SS and PTSA used for an additive are expected to have a similar effect on the growing surface. A molecule of SS or PTSA, which is adsorbed on active sites, appears to pin the surface movement by interruption of the movement of adatoms to the active sites.

In the dynamic scaling theory [13-14], the moving rate of the surface in the statistical surface growth model is described by two terms, one independent of the quenched noise and the other affected by the quenched noise. From the analogy, the internal stress  $\sigma(i, h, c)$  in the nickel thin film generated from the solution including SS or PTSA may be described by

$$\sigma = \sigma(i, h, c) \sim \sigma_0(i, h) + \sigma_1(c)h^{-p(c)}, \quad (2)$$

where  $\sigma_0(i, h)$  (which corresponds to Eq. (1)) is the internal stress free of the additive,  $i$  is the current density,  $h$  is the film thickness,  $c$  is the concentration of the additive,  $\sigma_1(c)$  ( $\sigma_1(c)=0$  at  $c=0$ ) means the translation of the internal stress, and  $p(c)$  is the exponent dependent on the concentration of the additive. The right-hand side in Eq. (2) indicates the equation comprising the first term independent of the quenched noise and the second term affected by the quenched noise. The second term that obeys the power law represents a deviation from the internal stress free of the additive.

#### 3.1 Internal stress measured at a fixed film thickness

Figure 1 shows the dependence of the internal stress at a film thickness of 1  $\mu\text{m}$  on the current density. The internal stress is translated in the minus direction parallel to the  $\sigma$ -axis with an increase in a concentration of SS or PTSA. The tensile internal stress changes into the compressive internal stress at a low current density.

We make an attempt to describe the decrease in the internal stress and shift from the tensile to the compressive stress owing to the additive. The film thickness of 1  $\mu\text{m}$  is chosen to ignore the exponent  $p(c)$  in Eq. (2). Using the data in Fig. 1, the value of  $\sigma_1(c)$  is determined by a minimized

difference between  $\sigma_o(i,h)$  and the internal stress  $\sigma(i,h,c)$  translated in a plus direction parallel to the  $\sigma$ -axis by addition of arbitrary  $\sigma_1(c)$ .

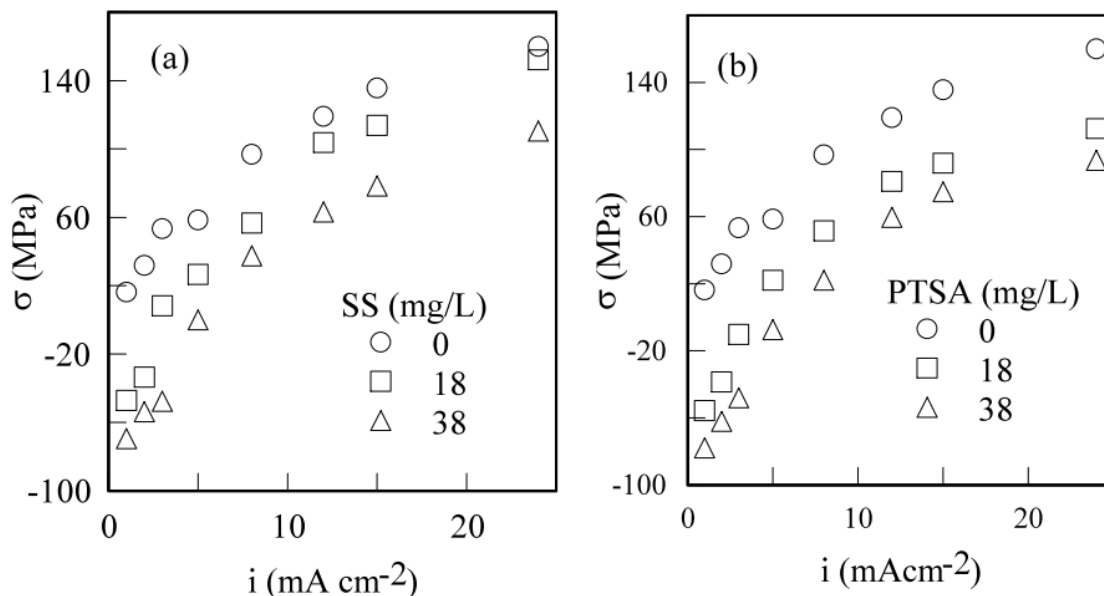


**Figure 1.** A plot of the internal stress vs. the current density in the nickel thin film 1 $\mu$ m thick electrodeposited from a solution including (a) SS and (b) PTSA. The internal stress in the nickel thin film electrodeposited from a solution free of the additive is shown as a reference.

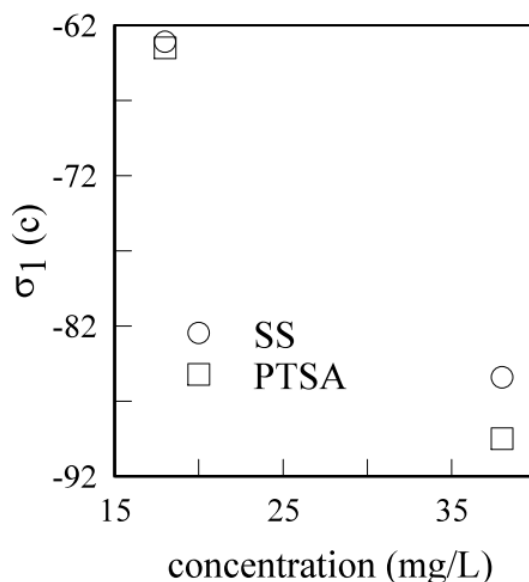


**Figure 2.** A plot of  $\sigma_1(c)$  vs. the concentration of the additive.

Figure 2 shows the dependence of  $\sigma_1(c)$  on the concentration of SS and PTSA. The sign of  $\sigma_1(c)$  is a negative value that indicates the compressive internal stress. The additive in this study decreases the internal stress as well as that in the previous studies [8-11]. The decrease in the internal stress with the addition of SS and PTSA may be explained by the incorporation of some point defect

into grain boundaries, for example, a sulfur atom. Point defects in the deposited thin film cause a compressive internal stress [16], whereas the grain boundary is the origin of tensile stress [1]. Sulfur atoms generated from SS were reported as a substitutional atom that causes a compressive internal stress and reduces the grain boundary energy [17].

3.2 Internal stress measured at a fixed current density

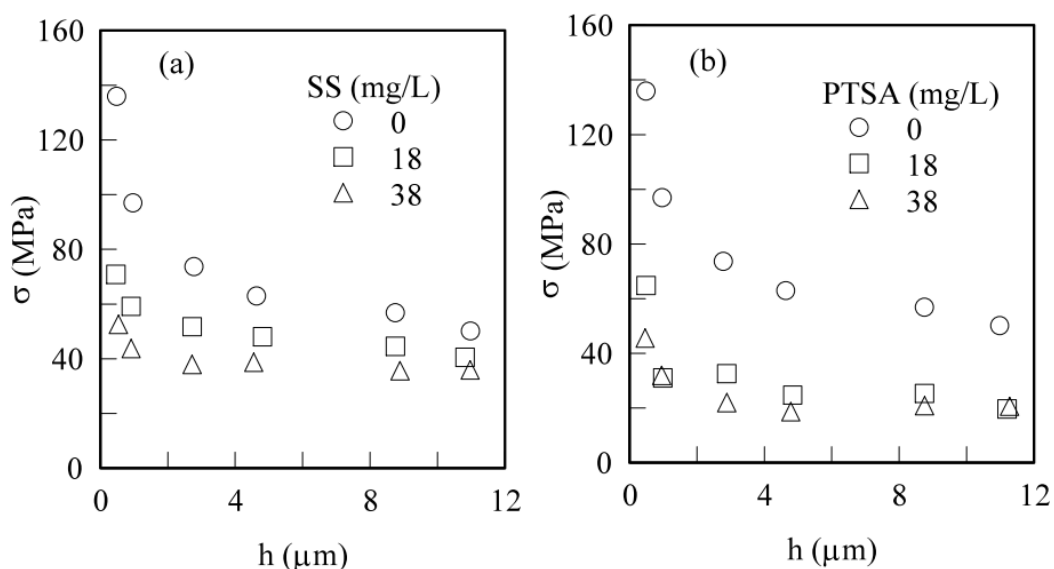


**Figure 3.** A plot of the internal stress vs. the film thickness in the nickel thin film electrodeposited at a current density of  $8 \text{ mA cm}^{-2}$  from a solution including (a) SS and (b) PTSA. The internal stress in the nickel thin film electrodeposited from a solution free of the additive is shown as a reference.

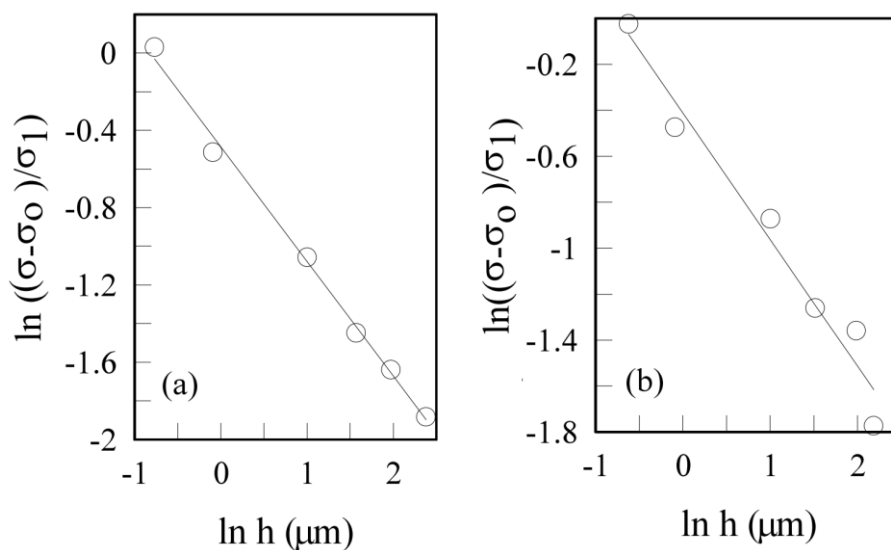


**Figure 4.** A log-log plot of  $(\sigma - \sigma_0) / \sigma_1$  vs. the film thickness for a solution including (a) 18 mg/L SS and (b) 38 mg/L SS. The slope best fitted to the data yields a value of  $p(n)$  in Eq. (2).

Figure 3 shows the effect of SS and PTSA on the internal stress in the nickel film electrodeposited at a current density of 8 mA cm<sup>-2</sup>. The tensile internal stress in the nickel film definitely decreases with a concentration of SS and PTSA. The internal stress in the nickel thin film electrodeposited at a higher concentration of SS and PTSA shows a weak dependence on the film thickness.

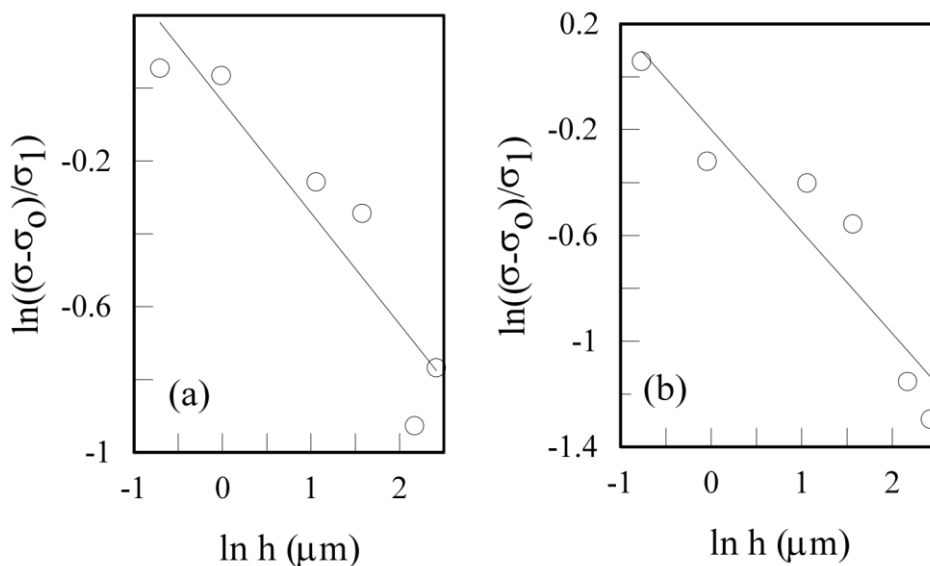


**Figure 5.** A log-log plot of  $(\sigma - \sigma_0) / \sigma_1$  vs. the film thickness for a solution including (a) 18 mg/L PTSA and (b) 38 mg/L PTSA. The slope best fitted to the data yields a value of  $p(n)$  in Eq. (2).

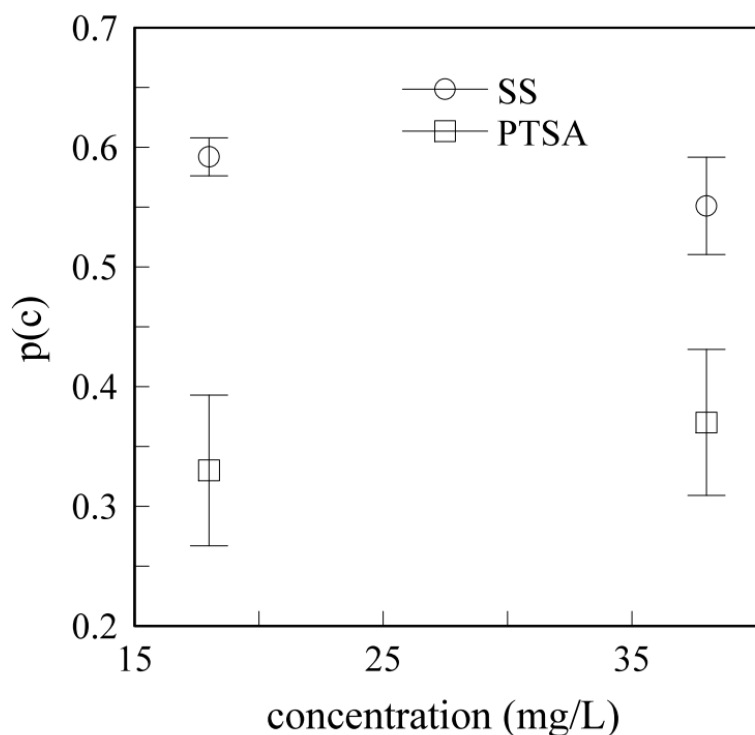


**Figure 6.** A plot of  $p(c)$  vs. the concentration of the additive.

According to the statistical surface growth model considering the quenched noise, the value of the scaling exponent is affected by the quenched noise. A log-log plot of  $(\sigma - \sigma_0) / \sigma_1$  vs. the film thickness at a SS concentration of 18 and 38 mg/L is shown in Fig. 4. According to Eq. (2), the slope of the straight-line best fitted to the data yields a value of  $p(n)$ .

In a similar way, a log-log plot of  $(\sigma - \sigma_0) / \sigma_1$  vs. the film thickness at a PTSA concentration of 18 and 38 mg/L is shown in Fig. 5.

In Fig. 6, the scaling exponent  $p(n)$  shows a weak dependence of the concentration of the additives. The value of  $p(n)$  for PTSA is smaller than that for SS. As the exponent  $n$  in Eq. (1) characterizes the dynamics of growth process, the value of  $p(c)$  is also considered to relate the dynamics of growth process such as the diffusion of nickel atoms. The smaller value of  $p(c)$  for PTSA indicates that nickel atoms in surface growth diffuse with a longer distance in the surface [5].

Thus, we can summarize the effect of the additive on the internal stress as  $\sigma(i, h, c) \sim \sigma_0(i, h) + \sigma_1(c)h^{-p(c)}$ .

### 3.3 Texture of the nickel thin film

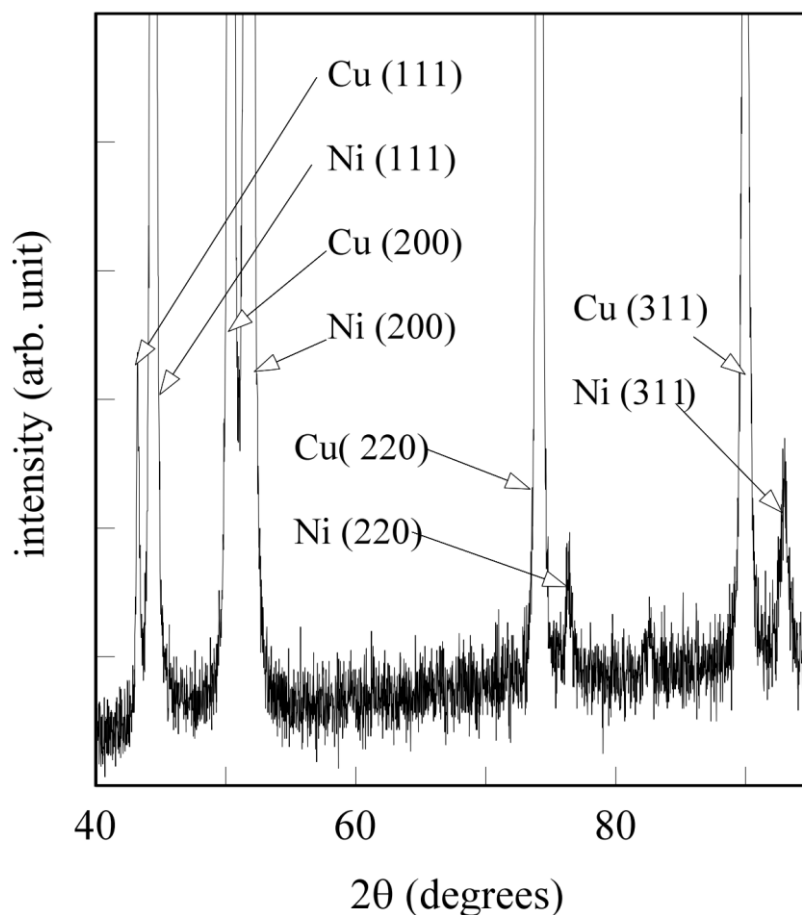


**Figure 7.** A typical XRD chart of the nickel thin film of 2.7 μm in thickness electrodeposited at a current density of 8 mA cm<sup>-2</sup> using 58 mg/L SS solution. The diffraction peaks of the nickel thin film and copper specimen were observed.

Our interest lies in a relationship between a preferential crystallographic plane in the nickel thin film and the elastic strain energy, which is directly observed as the internal stress. In X-ray analysis, a preferential growth plane in thin films is often evaluated by the texture coefficient [18]  $T(hkl)$  defined by

$$T(hkl) = \frac{I(hkl)_i / I_o(hkl)_i}{\sum_N I(hkl)_i / I_o(hkl)_i}, \quad (3)$$

where  $I(hkl)_i$  is the measured intensity of the  $(hkl)$  diffraction,  $I_o(hkl)_i$  is the standard intensity [19] of polycrystalline nickel, and  $N$  is the total number of a diffraction peak.

In FCC (face-centered cubic) metal films [20], the (100) plane has the lowest elastic strain energy, and the (111) plane has the lowest surface energy. The crystallographic plane that emerges in electrodeposition should lower the total formation energy comprising the surface energy and elastic strain energy including the grain boundary energy.

Figure 7 shows a typical XRD chart of the nickel thin film 2  $\mu\text{m}$  thick shows diffraction peaks of nickel comprising (111), (200), (220), and (311) diffraction. The nickel thin film was electrodeposited using the solution including 58 mg/L SS. The intensity in Eq. (3) was calculated using the Gaussian function [4] fitted to the diffraction peak in Fig. 7.

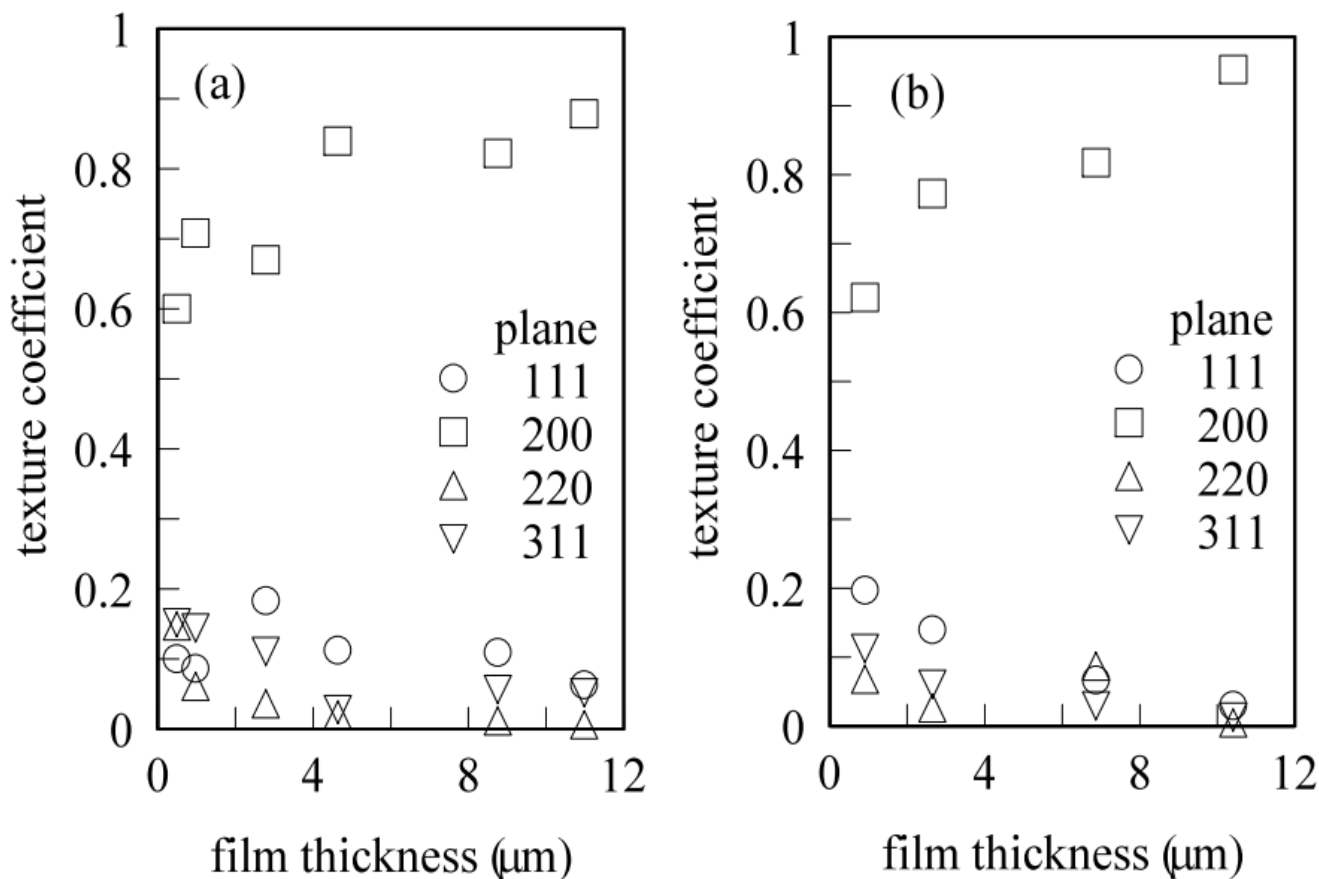


**Figure 8.** A plot of the texture coefficient vs. the film thickness from four different crystallographic planes with the low Miller index for (a) a solution free of SS and (b) a solution of 58 mg/L SS.

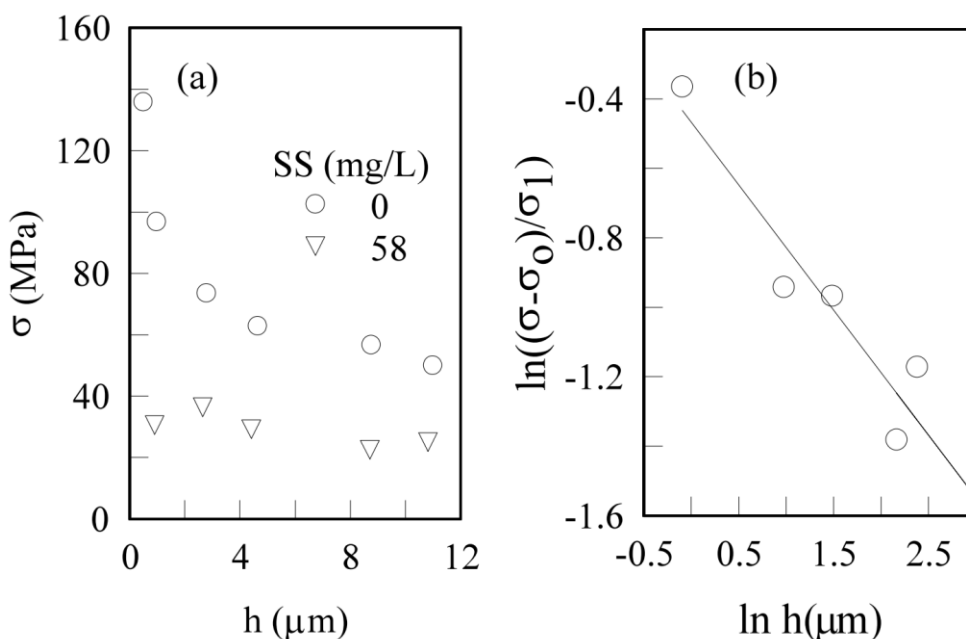


**Figure 9.** A scaling behavior of the internal stress in the nickel film electrodeposited at a current density of  $8 \text{ mA cm}^{-2}$  from 58 mg/L SS solution. (a) A plot of the internal stress vs. the film thickness. (b) A log-log plot of  $(\sigma-\sigma_0)/\sigma_1$  vs. the film thickness. The slope yields a value of  $p$  (c) =  $-0.36 \pm 0.06$ .

Figure 8 shows the texture coefficient for two kinds of SS concentrations, (a) 0 and (b) 58 mg/L. In the nickel thin film electrodeposited at a current density of  $8 \text{ mA cm}^{-2}$  from the solution of 0 and 58 mg/L, the (100) plane is found to be a dominant crystallographic plane parallel to the specimen as well as that in a previous study [21]. This indicates that the (100) plane emerges so as to lessen the total formation energy because the elastic strain energy is dominant in the nickel thin film. In a concentration range of SS in this study, the SS molecule that acts as the quenched noise in the (100) plane does not cause a change in the texture coefficient.

In addition, the internal stress in the nickel film electrodeposited at a current density of  $8 \text{ mA cm}^{-2}$  from a higher solution of SS, 58 mg/L was investigated whether it obeys Eq. (2) or not. Figure 9 (a) shows the dependence of the internal stress on the film thickness. Using  $\sigma_1(c) = -95.5$  extrapolated from the data in Fig. 2,  $p(n)$  is found to have a value of  $-0.36 \pm 0.06$  at a SS concentration of 58 mg/L as shown in Fig. 9 (b). This is approximately the same value as the value of  $p(c)$  at a PTSA concentration of 38 mg/L.

#### 4. CONCLUSIONS

We have investigated the internal stress affected by the quenched noise using the bent strip measurement. In the nickel thin film electrodeposited from the solution including SS and PTSA, the effect of the additive on the internal stress is shown to be equivalent to the quenched noise in the

dynamic scaling theory. The change in the internal stress due to the additive takes place in the (100) plane, according to the texture coefficient shown by XRD. The internal stress is found to be described by the unified equation comprising the power law,  $\sigma(i, h, c) = \sigma_0(i, h) + \sigma_1(c)h^{-p(c)}$ .

#### ACKNOWLEDGEMENTS

This work is supported by Grant-in-Aid for Scientific Research (C), No. 22560025 by the Ministry of Education, Science, and Culture of Japan. The author deeply appreciates Mr. M. Z. Azmir and T. Oshiro for their help in the experimental setup.

#### References

1. H. Windischmann, *Critic. Rev. Solid St. Mater. Sci.*, 17 (1992) 547.
2. M. Ghorbanpour and C. Falamaki, *J. Nanostructure chem.*, 3 (2013) 66.
3. Y. Li, H. Jiang, W. Huang, and H. Tian, *Appl. Surf. Sci.*, 254 (2008) 6865.
4. M. Saitou, *Int. J. Electrochem. Sci.*, 10 (2015) 5639.
5. A. -L. Barabási and H. E. Stanley, *Fractal Concepts in Surface Growth*, Cambridge Uni. Pr., New York (1995).
6. J. W. Dani, *Electrodeposition*, Noyes Pub., Newjersy (1993).
7. M. Schlesinger and M. Paunovic, *Modern Electroplating*, John Wiley & Sons, New York (2000).
8. M. Y. Popereka and V. V. Koshmanov, *Soviet Mater. Sci.*, 2 (1968) 453.
9. L. Oniciu and L. Mureşan, *J. Appl. Electrochem.*, 21 (1991) 565.
10. K. Boto, *Electrodeposition and Surface Treatment*, 3 (1975) 77.
11. J. -C. Hsu and K. -L. Lin, *Thin Solid Films*, 471 (2005) 186.
12. C. Lee and J. M. Kim, *Physica A*, 316 (2002) 144.
13. G. Costanza, *Physica A*, 330 (2003) 421.
14. S.V. Buldyrev, A. -L. Barabási, F. Caserta, S. Havlin, H. E. Stanley, and T. Vicsek, *Phys. Rev. A*, 45 (1991) R8313.
15. J. P. Stokes, A. P. Kushnick, and M. O. Robbins, *Phys. Rev. Lett.*, 60 (1988)1386.
16. S. J. Hearne and J. A. Floro, *J. Appl. Phys.*, 97 (2005) 014901.
17. A. Bhandari, S. J. Hearne, B. W. Sheldon, and S. K. Soni, *J. Electrochem. Soc.*, 156 (2009) D279.
18. S. Karim, M. E. T-Molares, F. Maurer, G. Miehe, W. Ensinger, J. Liu, T. W. Cornelius, and R. Neumann, *Appl. Phys. A*, 84 (2006) 403.
19. JCPDS-ICDD Card No. 04-850.
20. M. -Y. Cheng, K. -W. Chen, T. -F. Liu, Y. -L. Wang, and H. -P. Feng, *Thin Solid Films*, 518 (2010) 7468.
21. S. -H. Kim, H. -J. Sohn, Y. -C. Joo, Y. -W. Kim, T. -H. Yim, H. -Y. Lee, and T. Kang, *Surf. Coat. Technol.*, 199 (2005) 43.